Properties of Copolymer-Type Polyacetal/Ethylene–Propylene–Diene Terpolymer Blends

WEN-YEN CHIANG* and CHI-YUAN HUANG

Department of Chemical Engineering, Tatung Institute of Technology, 40, 3rd Sec., Chung Shang N. Road, Taipei 10451, Taiwan, Republic of China

SYNOPSIS

Two kinds of polymer blends, polyacetals (POMs) and ethylene–propylene–diene terpolymer (EPDM), have been prepared by mechanical blending. The rubbery EPDM was added to the rigid POM matrix to increase toughness. The mechanical, physical, thermal, dynamic mechanical, and morphological properties of these samples have been measured. The notched Izod impact strength and the elongation of the blends reaches a maximum at 7.5 wt % EPDM content. Scanning electron micrographs (SEM) showed that the domain sizes of EPDM vary from 0.25 to 1.0 μm and were independent of the composition. The POM/EPDM blends were determined to be immiscible by SEM, but showed single T_g behavior as determined by differential scanning calorimetry (DSC) and dynamic mechanical analyses up to 7.5 wt % EPDM. Because of that, the T_g's of POM and EPDM were very similar in value. © 1993 John Wiley & Sons, Inc.

INTRODUCTION

Two-phase polymeric systems, such as polyblends, are important in at least in two major areas of application: (1) A rubbery phase is added to a brittle polymer to increase toughness and the elongation at breakpoint of the brittle polymer.[1-5] (2) A rigid phase is added to a rubber to increase its strength and decrease its tendency to flow or to undergo permanent deformation under a load.[6-8] Polymer blends have received a lot of attention in recent years due to the possibility of obtaining compounds with novel and/or different properties through proper marriage of the properties of the respective components. Polyacetals (POMs) are strong, hard, highly crystalline thermoplastics. Product developments have been concerned with improving the flow and other properties of POM. A number of POM blends have been studied.[1,9-20] Elastomer-modified formulations are the most interesting POM development because the toughness of POM is markedly increased, without a significant effect on typical POM properties.

This work uses melt blending to make toughened POM. It also investigates the properties of various compositions of POM/ethylene–propylene–diene (EPDM) systems.

EXPERIMENTAL

Materials

Two commercial copolymer-type polyacetals (POMs), Duracon M90 and Duracon M270 (Japan Polyplastics Co.), with melt-flow indexes of 8.0 for M90 and 25.0 for M270, and one commercial ethylene–propylene–diene terpolymer (EPDM), Keltan 520 (DSM Chemical Co., Netherlands) were used. Keltan 520 contains a weight ratio of 55E/40.5P/4.5 dicyclopentadiene (DCPD).

Melt Blending

The variety of compositions of POM/EPDM were compounded at the weight ratios of 100/0, 97.5/2.5, 95.0/5.0, 92.5/7.5, 90/10, 85/15, 80/20, 70/30, and 50/50 and blended in the Brabender Plasti-corder Model PLE330 at 180°C for 8 min at 50 rpm. Test pieces were prepared by compression molding in a

* To whom correspondence should be addressed.

Journal of Applied Polymer Science, Vol. 47, 105–112 (1993)
 CCC 0021-8995/93/010105-08

frame at 150 kg/cm^2 for 6 min, and then they were cooled by a water-cooling system.

Mechanical Properties

Tensile properties were measured according to the ASTM D638 test method using the Instron Universal Testing Machine Model 1130. The thickness of the test specimen was 0.3 ± 0.02 cm. The crosshead load was 500 kg, at a speed of 5 cm/min, and the chart speed was 100 cm/min. The elastic modulus was determined from the initial part of the slope of the stress–strain curve within the linear trend. The values obtained were the averages of many measurements. Notched Izod impact strength was measured according to the ASTM D256 test method. The thickness of the impact test specimen was 0.3 ± 0.02 cm and the energy of hammer was 60 kg-cm.

Thermal Properties

A DuPont Instrument Analyzer 1090B equipped with a 910 differential scanning calorimeter (DSC) was used at a heating rate of 20°C/min to measure the T_g's. The thermogravimetric analyzer (TGA) 951 was used under nitrogen at a heating rate of 20°C/min to measure the thermal degradation of the blends.

X-ray Measurements

Wide-angle X-ray diffractograms (WAXD) were measured at room temperature on the Rigaku D/MAX-IIIA X-Ray diffractometer with FeKα radiation generated at 40 kV and 20 mA. The scan rate used for the WAXD profiles was 1°/min. A teletype was connected to the terminal of the digital counter so that the counts were automatically recorded. The degree of crystallinity (X_c) of the POM/EPDM blends was calculated from the diffraction peak by determining the ratio of the crystalline area to the total area; therefore, the X-ray diffraction from a two-phase model is assumed to be additive. The diffracted intensity is

$$X_c\,(\%) = (I_c/I) \times 100\%$$

where X_c is the crystallinity of the POM/EPDM blends; I_c, the intensity area between 2θ (Bragg angle) = 27° and 30°; and I, the intensity of the total area from 2θ = 19° to 35°.

The degree of crystallinity of the POM contained in POM/EPDM blends is expressed by following equation:

$$X_{c\,\mathrm{pom}}\,(\%) = (I_c/I \times W) \times 100\%$$

where $X_{c\,\mathrm{pom}}$ is the degree of crystallinity of the POM in POM/EPDM blends and W is the wt % of the POM in POM/EPDM blends.

Density Measurements

The density was measured according to the ASTM D792 test method. The calculation method has been described in previous papers.[1,21]

Hardness Test

Hardness was measured by the Rockwell hardness tester. The ASTM D785 testing procedure for the Rockwell method imposes specific times for each stage of the testing procedure. The indenter is initially forced into the material under a minor load of 10 kg for 10 s followed by a major load of 60 kg applied for 15 s. The reading is taken 15 s after the removal of the major load. The data are in units of Rockwell hardness (R score).

Dynamic Mechanical Measurements

The dynamic mechanical data, loss tangent (tan δ), and complex modulus E^* were obtained with the Rheovibron Dynamic Viscoelastomer (Model DDV-II-C) at a heating rate of 1–2°C/min and 110 Hz from −120 to 130°C. The correction due to clamp extension was applied at all temperatures.

SEM Photographs

To examine the phase morphology, compression-molded Izod bars were immersed in liquid nitrogen and fractured. These fractured surfaces were coated with gold and viewed end-on by a Cambridge Stereoscan S4-10 scanning electron microscope.

RESULTS AND DISCUSSION

Mechanical Properties

In the POM/EPDM blends, the EPDM weighed up to 50% of the total blend weight. The stress–strain properties of the POM/EPDM blends depend on the composition. The tensile strength, Young's modulus, elongation, and impact strength all vary with the composition. The rubbery EPDM was added to the rigid POM matrix to increase toughness and the elongation of POM's breakpoint. When

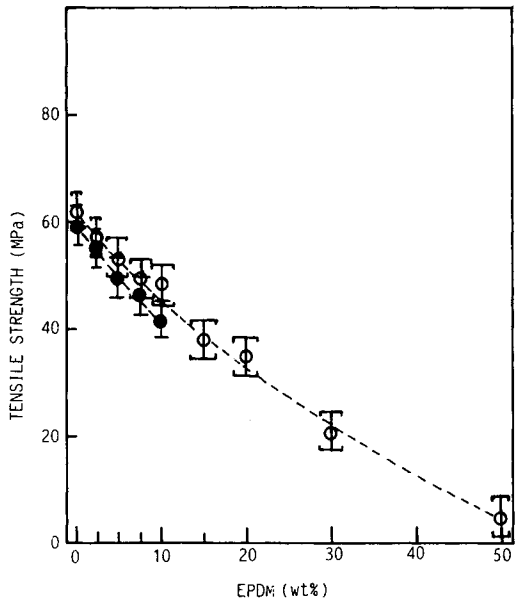

Figure 1 The tensile strength of POM/EPDM blends: (○) M90/EPDM; (●) M270/EPDM.

tensile strength is the function of the composition as plotted in Figure 1, the tensile strength of the POM/EPDM blends decreases with increasing EPDM content. The elongation of the blends reaches a maximum at 7.5 wt % EPDM content (Fig. 2). Because the degree of crystallinity in the blends decreases with increasing concentration of EPDM, the Young's modulus of the blend decreases in Figure 3. The addition of small amounts of one polymer to the other may result in improved structural homogeneity of the polymer and increased strength.[22-24] The variation of the strength of small additives was explained by the fact that the additives act as a damper in the redistribution of the internal stresses or that they fill some defects in the microstructure of the bulk polymers. However, a detailed study of the property changes of the polymers due to small additions of other polymers has not been fully reported to date and the mechanism of their effect remains unclear.[11] Lipatov[25] thought that the mechanical characteristics were connected to the interpenetration of the additive component into the surface defects of the bulk component. It is known that tensile strength of toughened plastic decreases with rubber content, whereas elongation at break increases with a certain range of rubber content. Figures 1–3 show that the POM/EPDM blends studied in this work followed this rule.

In POM/EPDM blends where the EPDM is in the dispersion phase and the POM is the matrix, the impact resistance is improved by the induced crazing of the POM or by the increased energy absorption during impact. It is well known that the effectiveness when toughening plastics with rubber depends on the shape, size, and the distribution of the rubber particles.[26-28] The impact strength vs. composition was plotted as shown in Figure 4. Yang et al.[3] suggested that in notched specimens there are macrocracks or macroflaws already present. Such

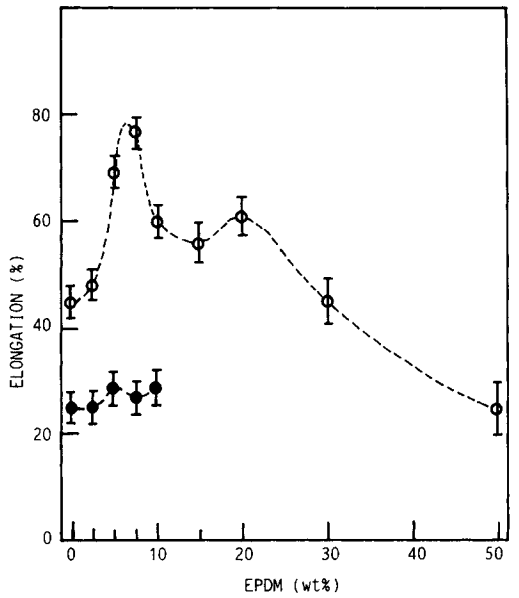

Figure 2 The elongation of POM/EPDM blends: (○) M90/EPDM; (●) M270/EPDM.

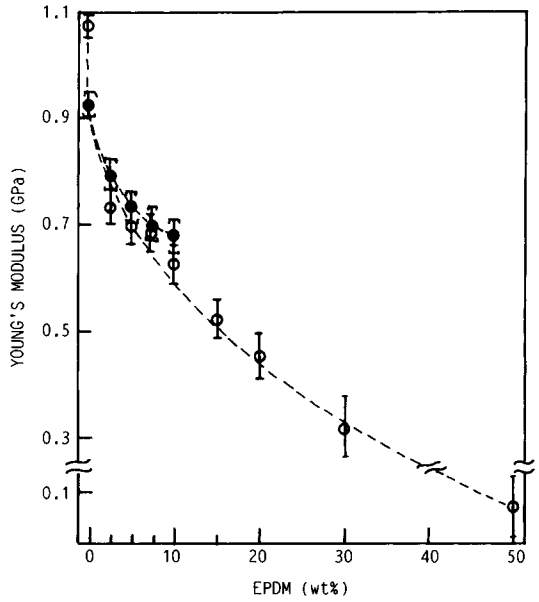

Figure 3 The Young's modulus of POM/EPDM blends: (○) M90/EPDM; (●) M270/EPDM.

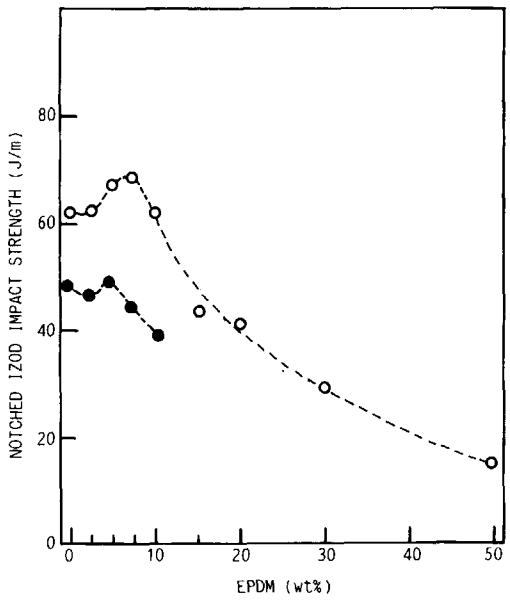

Figure 4 Notched Izod impact strength of POM/EPDM blends: (○) M90/EPDM; (●) M270/EPDM.

specimens require more numerous and larger rubber particles to stop microcrack propagation.[3] On the other hand, the rubber-matrix adhesion can be an important factor in determining the toughness of a rubber-toughened polymer. In polymer/rubber blends, rubber particles act as stress concentrators so that a tremendous number of craze cracks first start near the equator of the particle approximately perpendicular to the stress.[29] To produce a polyblend with high impact strength, there should be good adhesion between the two phases.[29] Therefore, the craze termination mechanism fails when the bond between the rubber and the matrix is weak. Instead of stabilizing the craze, a weakly bonded rubber particle pulls away from the matrix, leaving a hole in which the craze can propagate further, resulting in the breakdown of the craze and the possible formation of a crack.

This effect is similar to the effect that was observed with the glass beads. When there is good adhesion between the rubber and the surrounding matrix, the fracture surfaces reveal fractured rubber particles that have two halves along the equatorial plane. In POM/EPDM blends, this phenomenon did not occur. From the SEM, it was found that the particle size of the EPDM that was dispersed in POM varied from 0.25 to 1.0 μm. It showed that the adhesion of the two phases was poor and the EPDM particles were too small to resist the cracks that developed. The impact strength (Fig. 4) and the elongation (Fig. 2) improvements are very modest compared to those generally observed with elastomer-toughened plastics.

X-Ray Diffraction Measurements

The X-ray diffraction scans of the polymer blends with weight fractions of EPDM ranging from 0 to

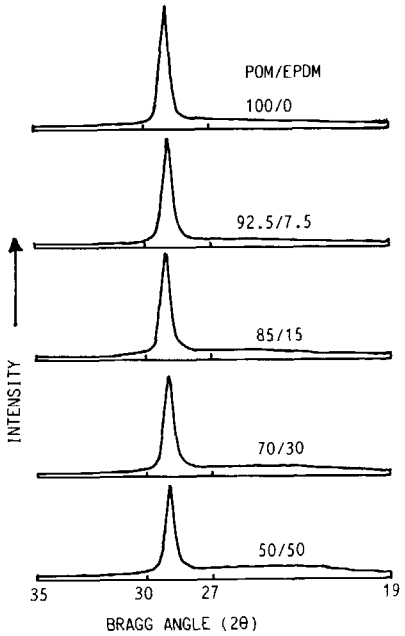

Figure 5 Radical intensity distribution of POM/EPDM blends.

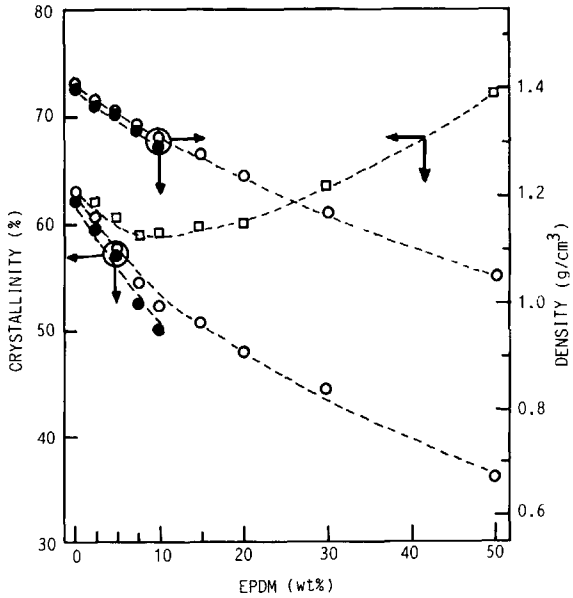

Figure 6 Crystallinity and density of POM/EPDM blends: (○) M90/EPDM; (●) M270/EPDM; (□) $X_{c\ pom}$ of M90/EPDM blends.

Table I Glass Transition Data for Blends of POM with EPDM

POM/EPDM	Damping Peak T_g (K)				
	Rheovibron			DSC	
100/0	202	–	375	229	—
92.5/7.5	210	–	375	231	—
70/30	202	223	375	229	241
0/100	—	223	—	—	241

50% as a function of the Bragg angle (2θ) are shown in Figure 5. For pure POM, a single sharp crystalline deflection peak at $2\theta = 28.8°$ can be observed. As the EPDM content increases, the crystalline diffraction peak becomes shorter; however, the position of the peak is independent of the composition, as expected. It is obvious that the unit cell dimensions of the POM remain unchanged. It has been suggested[30] that the EPDMs are amorphous in the unstretched state. From the diffraction curve of the POM/EPDM blends, the peak of the EPDM was not found. Therefore, we can say that Keltan 520 EPDM is an amorphous rubber. The degree of crystallinity and the density of the POM/EPDM blends decrease with increasing amounts of EPDM (Fig. 6). This is inevitable because the POM content of the POM/EPDM blends decreases with increasing EPDM content. However, the $X_{c\,pom}$ (Table I) of the POM(M90) that is contained in the POM/

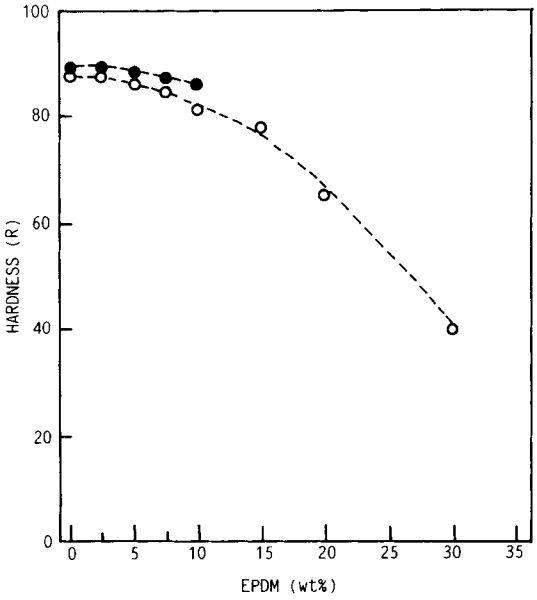

Figure 7 Hardness of POM/EPDM blends: (○) M90/EPDM; (●) M270/EPDM.

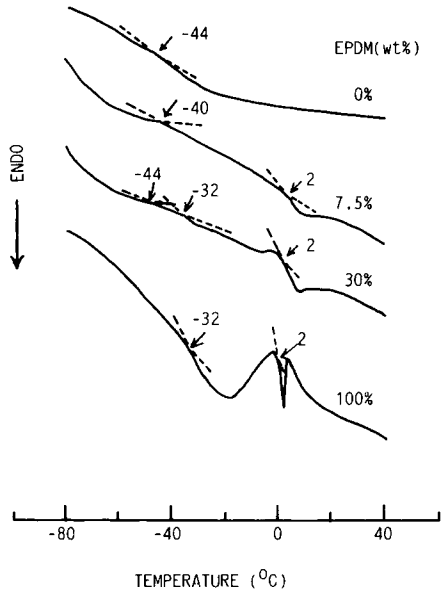

Figure 8 DSC trace for POM(M90)/EPDM blends.

EPDM blends reaches a minimum at 7.5 wt % EPDM content; i.e., at this composition, the POM of the POM/EPDM blend is less crystalline than are other POMs in the POM/EPDM blends. This is probably the reason that the POM(M90)/EPDM blends reach a maximum impact strength at 7.5 wt % EPDM content.

Hardness is essentially resistant to indentation and is a surface property in the strictest sense. Hardness testing of polymers involves all the major modes of mechanical behavior of polymers, i.e., elastic deformation, time-dependent plastic flow, retarded elastic deformation, and retarded elastic recovery.[31] In this work, the result of the hardness test is shown in Figure 7. It was found that the hardness of blends decreases slightly with increasing

Table II The X_c and $X_{c\,pom}$ of POM/EPDM Blends

POM/EPDM (wt %)	X_c (%)	$X_{c\,pom}$ (%)
100/0	63.2	63.2
97.5/2.5	60.5	62.0
95.0/5.0	57.5	60.5
92.5/7.5	54.5	58.9
90.0/10.0	53.4	59.3
85.0/15.0	50.7	59.6
80.0/20.0	48.0	60.0
70.0/30.0	44.4	63.4
50.0/50.0	36.0	72.0
0.00/100	0.0	0.0

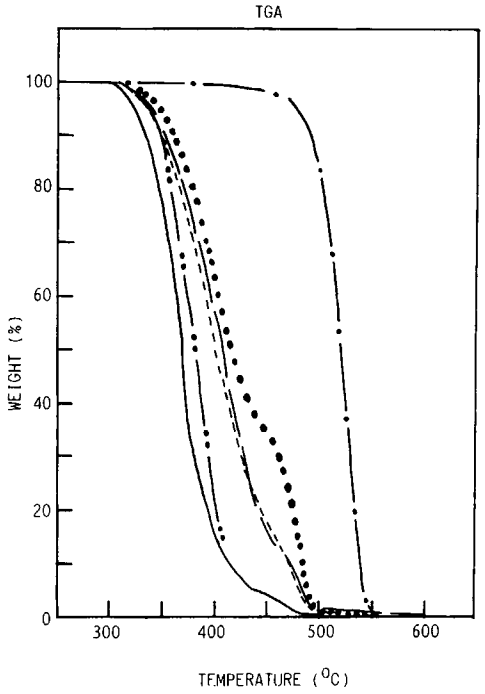

Figure 9 TGA diagram of POM(M90)/EPDM blends: (- · · -) POM; (—) 92.5/7.5; (------) 85/15; (– – –) 70/30; (· · · · · ·) 50/50; (– · –) EPDM.

concentration of EPDM below 7.5 wt % and then decreases sharply with an increasing content of EPDM.

Thermal Analysis

Figure 8 shows the thermogram scans of the POM(M90)/EPDM blends. From the figure, it was found that the glass transition temperature (T_g) is

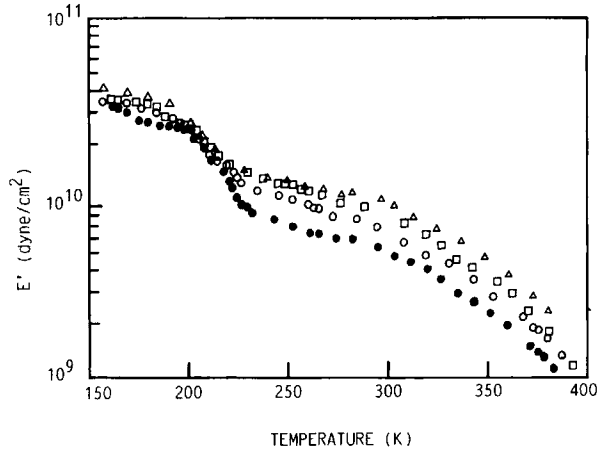

Figure 10 Storage modulus of POM(M90)/EPDM blends: (△) 100/0; (○) 92.5/7.5; (□) 85/15; (●) 70/30.

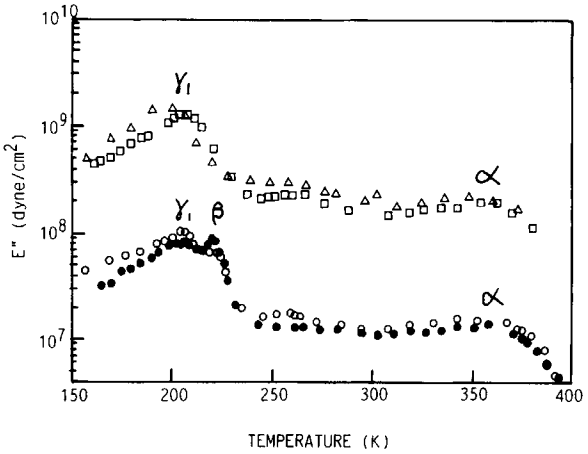

Figure 11 Loss modulus of POM/EPDM blends: (△) 100/0; (○) 92.5/7.5; (□) 85/15; (●) 70/30.

−44°C for POM and −32°C for EPDM. There is only one T_g, ca. −40°C, for the POM/EPDM (92.5/7.5) blends. However, there are two T_g's, −44 and −32°C, as the EPDM content was increased to 15 wt %. The results of the DSC test are summarized in Table II by showing the T_g observed for the POM and the EPDM phases of each blend.

Figure 9 compares the thermal stability of the blends by using the TGA diagram. As a result, the ranking of the thermal stability of the POM/EPDM blends are

EPDM > 30 wt % EPDM > 15 wt % EPDM > POM > 7.5 wt % EPDM

From the thermal stability ranking, it is known that the POM/EPDM (92.5/7.5) blend has the lowest thermal stability. This is because of the

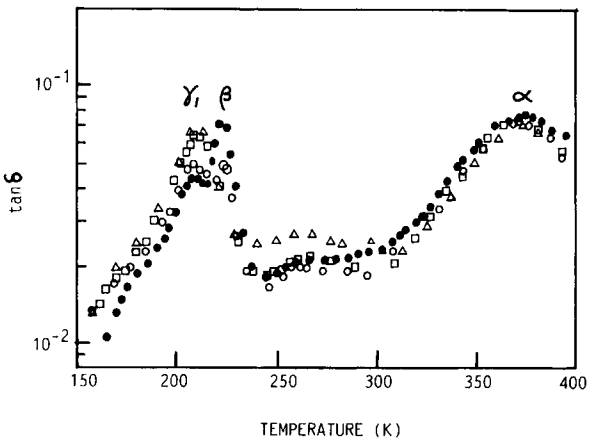

Figure 12 Loss tangent of POM/EPDM blends: (△) 100/0; (○) 92.5/7.5; (□) 85/15; (●) 70/30.

$X_{c\ pom}$ of the POM in the POM/EPDM (92.5/7.5) blend is lower than that of other POM/EPDM blends. Hence, the amorphous phase of the POM is greater than that of other blends, resulting in the POM/EPDM (92.5/7.5) blend having the lowest thermal stability.

Dynamic Mechanical Measurements

The POM/EPDM blend's storage modulus (E'), loss modulus (E″), and loss tangent (tan δ) curves vs. temperature are shown in Figures 10–12. Figure 10 shows that as the content of EPDM increases in the blends our first observation is a decrease in the modulus of the 92.5/7.5 POM/EPDM blend. Furthermore, as the content of EPDM increases, there is a marked decrease in the storage modules of the blends. The data in the Figure 11 show two prominent POM relaxation peaks, and these will be labeled α and $\gamma_1[T_g(L)]$ for the present discussion. The first peak occurs at 375 K (α transition). This was mentioned in Enns and Simha's[32] study. The second peak is a sharp transition at 202 K and is referred to as the γ_1 transition. It is the result of short segmental motions in the disordered regions.[33] Peak 223 K is the transition (β transition) of the EPDM. Figure 11 shows that there is only one glass transition temperature at 210 K for the POM/EPDM 92.5/7.5 blend. The T_g of the POM/EPDM blend 92.5/7.5 shifted at high temperature, ca. 8 K. Furthermore, there are two T_g's, γ_1 and β transitions, as the EPDM content increased to 15 wt %. Figure 12 shows that as the amount of EPDM increases there is a marked increase in the intensity of the β transition; however, the γ_1 damping peak is contrary. As a result, the POM/EPDM blends are immiscible systems. In PC/ABS[34] blends, the damping peak area ($T_{g\beta}$) is independent of the composition. This result is different from that of the POM/EPDM polymer blend.

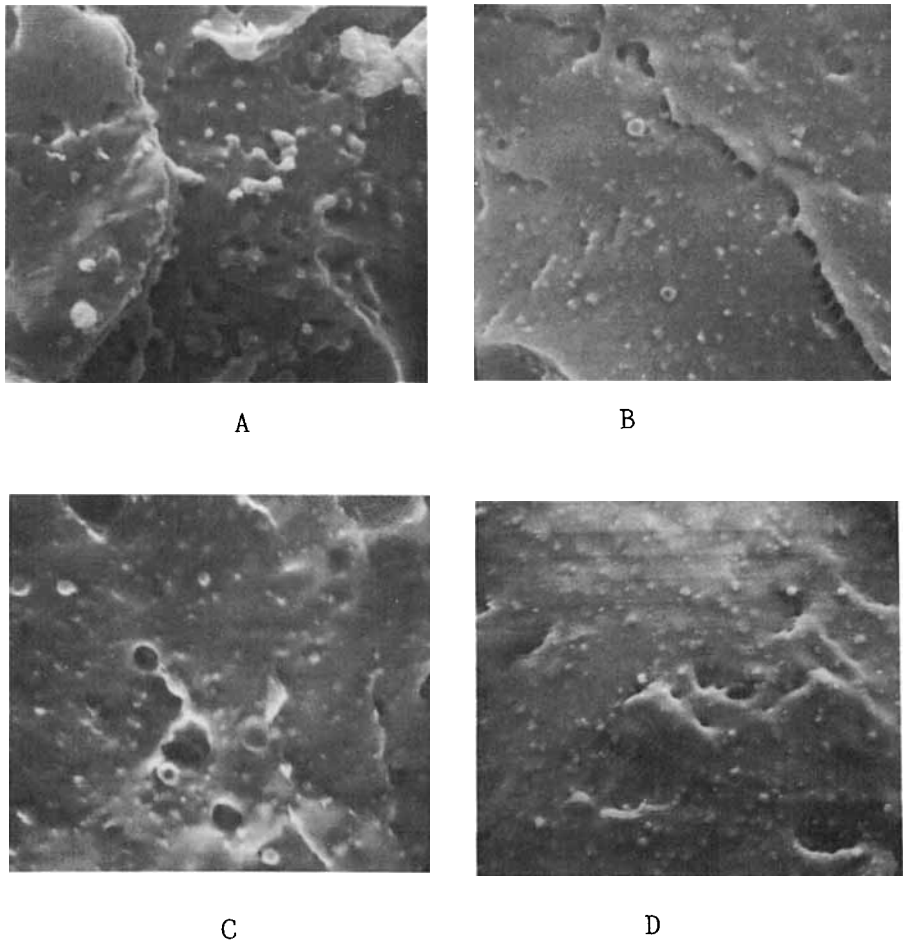

Figure 13 SEM photomicrographs of fractured surfaces of POM(M90)/EPDM blends: (A) 92.5/7.5; (B) 85/15; (C) 70/30; (D) 50/50.

Morphology

Figure 13 shows the morphology of the POM/EPDM blends, as observed by the SEM. It shows that the particle sizes of the dispersed EPDM range from 0.25 to 1.0 μm in diameter. The particle size of the EPDM in the POM/EPDM blends is independent of the composition. In this work, the N_c (compatibility number)[35] values vary from 0.015 (150 Å[35]/1.0 μm) to 0.06 (150 Å[35]/0.25 μm), where $N_c = \infty$ (compatible system); $N_c = 1$ (semicompatible system); and $N_c = 0$ (incompatible system). Thus, the blending system of this work is referred to as an incompatible system.

CONCLUSIONS

The mechanical, physical, thermal, dynamic mechanical, and morphological properties of polyacetal (POM)/ethylene–propylene–diene terpolymer (EPDM) blends with EPDM contents 0–50% by weight have been studied. The $X_{c\ pom}$ of the blends for 92.5/7.5 is lower than that of other blends. Maybe for this reason the notched Izod impact strength and elongation at break of the blends reach a maximum at 7.5 wt % EPDM content. The particle sizes of dispersed EPDM are independent of composition and vary from 0.25 to 1.0 μm. The blends were determined to be immiscible by scanning electron microscopy but showed single T_g behavior as determined by differential scanning calorimetry (DSC) and dynamic mechanical analyses up to 7.5 wt % EPDM. It was because of that that the T_g's of POM and EPDM were very similar in value.

The authors wish to express their appreciation to Dr. T. S. Lin, president of the Tatung Institute of Technology, for his encouragement and support.

REFERENCES

1. W. Y. Chiang and M. S. Lo, *J. Appl. Polym. Sci.*, **36,** 1685 (1988).
2. W. Y. Chiang and C. Y. Huang, *J. Appl. Polym. Sci.*, **38,** 951 (1989).
3. D. Yang, B. Zhang, Y. Yang, Z. Fang, G. Sun, and Z. Feng, *Polym. Eng. Sci.*, **24,** 612 (1984).
4. W. Y. Chiang and C. Y. Huang, *Ta-T'ung Hsueh Pao,* **19,** 97 (1989). *Chem. Abstr.*, **114,** 103343r (1991).
5. C. Domenici, G. Levita, A. Marchetti, and V. Frosini, *J. Appl. Polym. Sci.*, **34,** 2285 (1987).
6. K. Satake, *J. Appl. Polym. Sci.*, **14,** 1007 (1970).
7. J.-M. Charrier and R. J. P. Ranchoux, *Polym. Eng. Sci.*, **11,** 381 (1971).
8. W. Y. Chiu and T. C. Hsueh, *J. Appl. Polym. Sci.*, **32,** 4663 (1986).
9. T. I. Ablazova, M. B. Tsebrenko, and A. B. V. Yudin, *J. Appl. Polym. Sci.*, **19,** 1781 (1975).
10. Yu. Lipatov, *J. Polym. Sci. Polym. Symp.*, **61,** 369 (1977).
11. Yu. Lipatov, *J. Appl. Polym. Sci.*, **22,** 1895 (1978).
12. W. Y. Chiang and C. Y. Huang, *J. Chin. I. Ch. E.*, **22,** 291 (1991).
13. N. Klemmer and B. J. Jungnickel, *Colloid Polym. Sci.*, **262,** 381 (1984).
14. Yu. S. Lipatov, *Vysokomol. Soyed.*, **A20,** 3 (1978).
15. W. Y. Chiang and C. Y. Huang, *Angew. Makromol. Chem.*, **196,** 21 (1992).
16. Ye. V. Lebedev, Yu. S. Lipatov, and O. V. AnokHin, *Vysokomol. Soyed.*, **A23,** 1723 (1981).
17. Yu. S. Lipatov, A. Ye. Nesterov, T. D. Ignatova, V. F. Shumskii, and A. N. Gorbatenko, *Vysokomol. Soyed.*, **A24,** 549 (1982).
18. O. V. Romankevich, T. I. Zhila, S. Ye. Zabello, N. A. Sklyar, and S. Ya. Frenkel, *Vysokomol. Soyed.*, **A24,** 2282 (1982).
19. P. E. Bretz, *J. Appl. Polym. Sci.*, **27,** 1707 (1982).
20. E. A. Flexman, Jr., *Mod. Plast.*, **62,** 72, 74, 76 (1985).
21. W. Y. Chiang and M. S. Lo, *J. Appl. Polym. Sci.*, **34,** 1997 (1987).
22. V. Kargin, *Vysokomol. Soyed.*, **A13,** 231 (1971).
23. E. Lebedev, Yu. S. Lipatov, and V. Privalko, *Vysokomol. Soyed.*, **A17,** 148 (1975).
24. T. Sogolova, M. S. Akutin, and D. J. ZanKin, *Vysokomol. Soyed.*, **A17,** 2505 (1975).
25. Y. Lipatov, *Pure Appl. Chem.*, **43,** 273 (1975).
26. J. A. Manson and L. H. Sperlin, Eds., in *Polymer Blends and Composites,* Plenum Press, New York, 1976.
27. C. B. Bucknall, L. Holliday and A. Kelly, F.R.S., Eds., in *Toughened Plastics,* Applied Science, London, 1977.
28. J. Silberger and C. D. Han, *J. Appl. Polym. Sci.*, **22,** 599 (1978).
29. L. E. Nielsen, in *Mechanical Properties of Polymers and Composites,* Marcel Dekker, New York, 1974, Vol. 2.
30. I. W. Bassi, P. Corradini, G. Fagherazzi, and A. Valvassori, *Eur. Polym. J.*, **6,** 709 (1970).
31. P. J. Phillips and N. R. Ramakrishnan, *Polym. Eng. Sci.*, **18,** 869 (1978).
32. J. B. Enns and R. Simha, *J. Macromol. Sci. Phys.*, **B13,** 25 (1977).
33. R. T. V. Hojfors, E. Baer, and P. H. Geil, *J. Macromol. Sci. Phys.*, **B13,** 323 (1977).
34. W. Y. Chiang and D. S. Hwung, *Polym. Eng. Sci.*, **27,** 632 (1987).
35. D. S. Kaplan, *J. Appl. Polym. Sci.*, **20,** 2615 (1976).

Received July 14, 1991
Accepted March 3, 1992